AIP | The Journal of Chemical Physics

Vibrational energy transfer near a dissociative adsorption transition state: State-to-state study of HCl collisions at Au(111)

Jan Geweke, Pranav R. Shirhatti, Igor Rahinov, Christof Bartels, and Alec M. Wodtke

Citation: The Journal of Chemical Physics **145**, 054709 (2016); doi: 10.1063/1.4959968
View online: http://dx.doi.org/10.1063/1.4959968
View Table of Contents: http://scitation.aip.org/content/aip/journal/jcp/145/5?ver=pdfcov
Published by the AIP Publishing

Vibrational energy transfer near a dissociative adsorption transition state: State-to-state study of HCl collisions at Au(111)

Jan Geweke,[1,2,3,a)] Pranav R. Shirhatti,[1,3] Igor Rahinov,[4] Christof Bartels,[1,3,b)] and Alec M. Wodtke[1,2,3,5]

[1]*Department of Dynamics at Surfaces, Max Planck Institute for Biophysical Chemistry, 37077 Göttingen, Germany*
[2]*Max-Planck—EPFL Center for Molecular Nanoscience and Technology, Institute of Chemical Sciences and Engineering (ISIC), Station 6, École Polytechnique Fédérale de Lausanne, CH-1015 Lausanne, Switzerland*
[3]*Institute for Physical Chemistry, Georg-August University of Göttingen, 37077 Göttingen, Germany*
[4]*Department of Natural Sciences, The Open University of Israel, 4353701 Ra'anana, Israel*
[5]*International Center for Advanced Studies of Energy Conversion, Georg-August University of Göttingen, 37077 Göttingen, Germany*

(Received 26 May 2016; accepted 6 July 2016; published online 4 August 2016)

In this work we seek to examine the nature of collisional energy transfer between HCl and Au(111) for nonreactive scattering events that sample geometries near the transition state for dissociative adsorption by varying both the vibrational and translational energy of the incident HCl molecules in the range near the dissociation barrier. Specifically, we report absolute vibrational excitation probabilities for HCl($v = 0 \rightarrow 1$) and HCl($v = 1 \rightarrow 2$) scattering from clean Au(111) as a function of surface temperature and incidence translational energy. The HCl($v = 2 \rightarrow 3$) channel could not be observed—presumably due to the onset of dissociation. The excitation probabilities can be decomposed into adiabatic and nonadiabatic contributions. We find that both contributions strongly increase with incidence vibrational state by a factor of 24 and 9, respectively. This suggests that V-T as well as V-EHP coupling can be enhanced near the transition state for dissociative adsorption at a metal surface. We also show that previously reported HCl($v = 0 \rightarrow 1$) excitation probabilities [Q. Ran *et al.*, Phys. Rev. Lett. **98**, 237601 (2007)]—50 times smaller than those reported here—were influenced by erroneous assignment of spectroscopic lines used in the data analysis. *Published by AIP Publishing.* [http://dx.doi.org/10.1063/1.4959968]

I. INTRODUCTION

The Born-Oppenheimer approximation[1] (BOA) is widely used to construct potential energy surfaces (PESs) that are used to describe interatomic forces in simple gas-phase reactions.[2–5] A major challenge in extending this approach to surface chemistry is to properly describe the interaction between the reacting species and the solid upon which the reaction is occurring. This requires accounting for surface atom motion—the description of surface chemical reactions intrinsically requires a high dimensional PES.[6,7] In addition, there is copious evidence that electron-hole pairs (EHPs) can couple to the vibrational degrees of freedom of molecules colliding with a metal surface—a scenario that cannot be described within the BOA.[8] While methods for constructing full dimensional PESs for surface chemistry are rapidly advancing,[9–12] the inclusion of electronically nonadiabatic effects still is a major challenge. Understanding the structure and energetics of the transition state is essential for a proper description of a chemical reaction. If the influence of electronically nonadiabatic effects is particularly strong here, the reactivity will be severely affected. In this context, an important open question is: How important is the exchange of energy between nuclear motion and EHPs when geometries close to the reaction's transition state are reached?[13]

An experimental approach to answering this question is suggested by work on H_2 collisions at a Cu(111) surface. By controlling the incidence energy of the H_2 molecule to be close to that of the reaction barrier for dissociative adsorption, $H_2 \rightarrow 2H_{(ad)}$, it could be shown that vibrational excitation of $H_2(v = 0 \rightarrow 1)$ is strongly enhanced for trajectories that sample geometries similar to the structure of the transition state.[14,15] Here, the influence of the transition state on vibrational excitation can be understood in terms of an electronically adiabatic PES where the reaction is translationally and vibrationally promoted and the vibrational excitation probabilities increase with incidence translational energy.[16]

In this work, we studied the vibrational excitation of HCl in collisions with a clean crystalline Au(111) surface. Specifically, we report absolute probabilities for collision-induced HCl($v = 0 \rightarrow 1$) and HCl($v = 1 \rightarrow 2$) vibrational excitation as a function of surface temperature (T_S) and incidence translational energy (E_i). Similar to H_2 on Cu(111), HCl can dissociate on Au(111) over a reaction barrier (at $E_i > 1$ eV,[17] calculated barrier height: 0.65 eV[18,19]) and the reaction is strongly enhanced by vibrational excitation,[17] reflecting a possible late transition state.[18,20,21] Vibrational

a)Author to whom correspondence should be addressed. Electronic mail: jan.geweke@mpibpc.mpg.de
b)Present address: Institute of Physics, University of Freiburg, 79104 Freiburg, Germany.

energy transfer between HCl and the Au(111) surface proceeds by two different mechanisms: an electronically adiabatic and an electronically nonadiabatic one.[22,23] The adiabatic mechanism involves V-T coupling—as in the case of H_2/Cu(111)—whereas the nonadiabatic mechanism requires V-EHP coupling. Accordingly, the measured excitation probabilities can be decomposed into electronically adiabatic and nonadiabatic contributions. We find that both mechanisms of vibrational energy transfer get strongly enhanced when the total internal energy (vibration and translation) of the incident molecules is high enough to allow access to the dissociation barrier. We also observe that for the incident molecules, providing energy in the vibrational mode (as opposed to translation) is much more effective in promoting further vibrational excitation. A similar comparison of NO($v = 0 \rightarrow 1$) with NO($v = 2 \rightarrow 3$) vibrational excitation in collision with Au(111) (at $E_i = 0.41$ eV) shows that in this case the enhancement is much smaller. The NO/Au(111) system is well known for its strong electronically nonadiabatic vibrational energy transfer. However, the dissociation barrier (~3 eV[24]) is energetically not accessible under the conditions employed. Our results suggest that for HCl/Au(111) both V-T and V-EHP coupling are dramatically enhanced in the vicinity of the transition state for dissociative adsorption at a metal surface, even when the collision trajectory fails to pass over it. Extending this argument further, it might well be possible that the reactive trajectories, i.e., those that do pass over the transition state, are also influenced by nonadiabatic interactions. If this is true, then incorporating these effects will be essential to successfully model the reactivity of this system.

II. EXPERIMENTAL

A. Experimental overview

The gas-surface scattering apparatus used in this study was described in detail elsewhere[23] and only a brief description is provided here. The apparatus consists of four interconnected chambers. In the source chamber, a gas mixture of HCl seeded in H_2 was expanded in a supersonic jet from a home-built, solenoid-driven pulsed valve (8 bar backing pressure, 298 K operating temperature, 0.2 mm diameter orifice). The molecular beam passed through a 1.5 mm diameter skimmer and two differential pumping chambers with 3 mm and 2 mm diameter apertures, respectively, before entering the ultra-high vacuum scattering chamber (base pressure $\sim 2 \times 10^{-10}$ Torr). Here, the Au(111) surface (orientation accuracy better than 0.1°, purity 99.999%, MaTeck GmbH), mounted on a 4-axis (x, y, z, Θ) translation stage, was positioned approximately 180 mm away from the nozzle. Before every set of experiments, the surface was prepared by sputtering with Ar ions (3 keV, 20 min), followed by annealing at 1000 K for >60 min. Cleanliness of the surface was checked using Auger electron spectroscopy. Molecular beam pulses measured 15 mm in front of the Au(111) surface were 40 μs (FWHM) in duration. The mean incidence energy of the HCl molecules was varied from 0.64 eV to 1.06 eV by changing the HCl/H_2 mixing ratio.

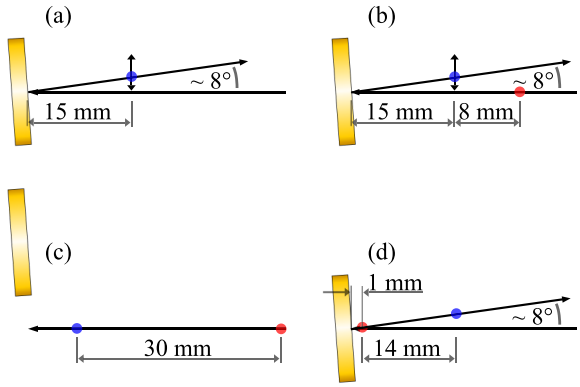

FIG. 1. Positions of the REMPI (blue) and the IR (red) beams relative to the surface and the travelling direction of the molecular beam (black arrows) which the laser beams intersect perpendicularly. For measuring $v = 0 \rightarrow 1$ excitation, molecules are detected 15 mm away from the surface (a). $v = 1 \rightarrow 2$ excitation requires the same REMPI position but the incident molecules are excited to $v = 1$ at a distance of 23 mm in front of the surface (b). Time-of-flight measurements are carried out with a flight distance of (c) 30 mm for the incident beam and (d) 14 mm for the scattered molecules. In the latter case, prior to collision the molecules are tagged with the IR close (1 mm) to the surface. Angular distributions are measured as in (a) and (b) by moving the REMPI beam along the vertical plane depicted by the vertical black arrows.

The experimental layout shown in Figs. 1(a) and 1(b) allowed determination of the vibrational excitation probabilities for HCl($v = 0 \rightarrow 1$) and HCl($v = 1 \rightarrow 2$), respectively. Incident HCl($v = 1$) molecules were produced by infrared (IR) excitation of HCl($v = 0$, $J = 0$) using the R(0) transition (red spots in Fig. 1). The IR laser system was comprised of a continuous wave (cw) Nd:YLF laser (Coherent Verdi V10) pumping a cw dye ring laser (Sirah Matisse DR, <20 MHz linewidth), whose output (~630 nm) was pulse-amplified in a five-stage Sirah Pulsed Amplifier 5×. The pulsed visible light was combined with the fundamental output (1064 nm) of an injection seeded Nd:YAG laser (Spectra-Physics Quanta Ray Pro 230) for difference frequency mixing in a $LiNbO_3$ crystal. The mid-IR output was parametrically amplified with the Nd:YAG fundamental to give IR pulses at a wavelength of ~3.4 μm with energies of ~5-7 mJ (see Ref. 25 for further information). In the absence of IR pre-excitation, only HCl($v = 0$) could be detected in the incident molecular beam. Using a (2 + 1) Resonance Enhanced Multi-Photon Ionization (REMPI) scheme, the population of each vibrational state HCl($v = 0,1,2$) was measured after scattering from the Au(111) surface by recording all observable ro-vibronic lines associated with the Q branch of the $E^1\Sigma^+ \leftarrow X^1\Sigma^+$ transitions; see Table I. The resulting ions were transported by a repeller and a collimating electrostatic lens onto a detector with two Multi-Channel Plates (MCPs) in Chevron configuration. To prevent errors arising from ion fragmentation (cf. Simpson *et al.*[26] and Rohlfing *et al.*[27]), signal from all ions (H^+, Cl^+, and HCl^+) was integrated. The observed REMPI signals were corrected for differences in MCP gain and variations in laser power, etc., measured independently in control experiments, and the vibrational excitation probabilities were calculated in a manner similar to that reported previously.[28]

Information about HCl translational energy distributions was obtained from state-to-state time-of-flight

TABLE I. Overview of the REMPI transitions and associated laser wavelengths (in air). All transitions are Q branch transitions from the given v and J states via $E^1\Sigma^+$ ($v = 0$).

J	$v = 0$ (λ/nm)	$v = 1$ (λ/nm)	$v = 2$ (λ/nm)
0	238.65	247.16	255.97
1	238.68	247.18	256.00
2	238.72	247.23	256.04
3	238.78	247.29	256.10
4	238.87	247.38	256.18
5	238.97	247.50	256.29
6	239.11	247.63	256.43
7	239.29	247.80	256.58
8	239.48	247.99	256.78
9	239.68	248.19	256.97

measurements.[25,29,30] Figs. 1(c) and 1(d) show the corresponding experimental setups. Incidence velocities were measured by exciting HCl($v = 0, J = 0$) into the $v = 1, J = 1$ state using the pulsed IR laser, state-specifically ionizing the excited molecules by REMPI at ~30 mm distance and recording the ion signal as a function of the delay between the two laser pulses. To obtain information about the translational energy distributions of scattered HCl molecules, the geometry of Fig. 1(d) was used. For example, incident HCl($v = 0$) molecules were pumped to their $v = 1, J = 1$ state with the IR beam at a position 1 mm from the surface prior to collision. HCl($v = 2$) produced by surface scattering was then detected by REMPI and scanning the delay again revealed the time-of-flight distributions (results are presented in Sec. II of the supplementary material).

B. Calibration of HCl vibrational state detection sensitivity

We require accurate knowledge of the relative state-specific REMPI detection sensitivities, which depend on the Franck-Condon factors, $Q(v_\Sigma, v)$, and rotational line strengths, $S(j_\Sigma, j)$, of the two-photon E-X transitions as well as the ionization cross-sections of the intermediate states, $\sigma_{v_\Sigma}(\lambda_v)$. Similar to experiments conducted by Simpson *et al.*,[26] we employed saturated IR pumping to produce well-defined population ratios of HCl in different vibration and rotation states; see Fig. 2. Here, REMPI-laser wavelength scans probed the incident HCl($v = 0$ and 1) populations with and without IR laser excitation, where the two laser beams were spatially and temporally overlapped. The REMPI signal depletion of the $v = 0$ state (shaded in Fig. 2(a)) is compared to the $v = 1$ REMPI signal enhancement (shaded in Fig. 2(b)). Given that the lifetime of this vibrationally excited state is long enough, the ratio of the magnitude of the $v = 1$ enhancement to the $v = 0$ depletion directly gives the relative REMPI detection sensitivity factor. Figs. 2(c) and 2(d) show examples of similar measurements of the relative detection sensitivity for HCl($v = 1$ and 2). Here, a heated nozzle operating at 1060 K was used to enhance the population of HCl($v = 1$) in the molecular beam.[17] This measurement protocol was repeated for several HCl rotational states populated in the molecular beam. The relative sensitivities were determined from the integrated, laser power corrected REMPI signals $I_v^{\mathrm{IR}}(J)$ as

$$\frac{\phi_{v=1}}{\phi_{v=0}} = \frac{S(J_\Sigma + 1, J + 1) \times Q(0_\Sigma, 1) \times \sigma_{0_\Sigma}(\lambda_1)}{S(J_\Sigma, \mathrm{J}) \times Q(0_\Sigma, 0) \times \sigma_{0_\Sigma}(\lambda_0)} \propto \frac{I_{v=1}^{\mathrm{IR:on}}(J+1)}{I_{v=0}^{\mathrm{IR:off}}(J) - I_{v=0}^{\mathrm{IR:on}}(J)} = 0.9 \pm 0.2 \quad (1)$$

and

$$\frac{\phi_{v=2}}{\phi_{v=1}} = \frac{S(J_\Sigma + 1, J + 1) \times Q(0_\Sigma, 2) \times \sigma_{0_\Sigma}(\lambda_2)}{S(J_\Sigma, J) \times Q(0_\Sigma, 1) \times \sigma_{0_\Sigma}(\lambda_1)} \propto \frac{I_{v=2}^{\mathrm{IR:on}}(J+1)}{I_{v=1}^{\mathrm{IR:off}}(J) - I_{v=1}^{\mathrm{IR:on}}(J)} = 0.5 \pm 0.1. \quad (2)$$

The uncertainties correspond to 95% confidence. No systematic dependence on J state could be observed (more details on the individual measurements can be found in Sec. I of the supplementary material). We also note that our value for $\phi_{v=2}/\phi_{v=1}$ is consistent with the relative detection sensitivity of 0.5 reported previously.[31]

C. A necessary correction to previous work

Absolute vibrational excitation probabilities for HCl($v = 0 \rightarrow 1$) transitions induced by molecular collisions at a Au(111) surface have been previously reported.[22] Surprisingly, those values are about 50 times smaller than the results that we report here. We attribute this discrepancy to incorrect spectroscopic assignments, resulting in erroneous detection sensitivity factors for $v = 0$ and 1 used in the previous work. There, the authors believed to have identified REMPI signal

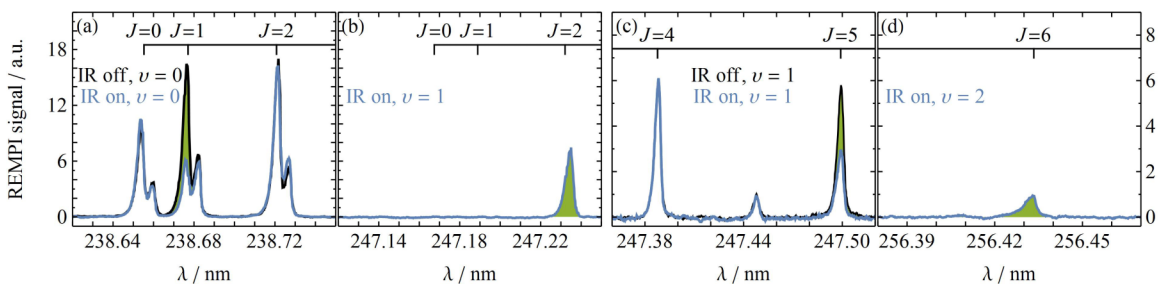

FIG. 2. REMPI spectra of incident HCl molecules (a) in $v = 0$ and (c) in $v = 1$ with and without IR pumping the R(1) and R(5) transition (blue and black curves), respectively. In (b) and (d), the respective upper state in $v = 1$ and $v = 2$ with IR on is shown (blue curve). All spectra in connected panels were recorded with the same laser power and detector gain. The intensity losses in (a) and (c) as well as the gains in (b) and (d) are illustrated by the green-shaded areas. Their ratios yield the relative sensitivity factors $\phi_{v=1}/\phi_{v=0}$ and $\phi_{v=2}/\phi_{v=1}$ which were measured for several J states (see Sec. I of the supplementary material).

from HCl($v = 1$) in the incident beam. Since the nozzle was held at room temperature and vibrations do not relax efficiently in an expansion, it was assumed that this population was equal to room-temperature thermal population. Based on this assumption, the line intensities were used to obtain REMPI sensitivity factors for $v = 0$ and 1. This implied approximately 45 times higher REMPI sensitivity for HCl($v = 1$) than for HCl($v = 0$). By contrast, our relative sensitivity factor for $v = 0$ and 1 is close to unity. We investigated this further and found that the weak transitions identified in the incident beam in that work were not due to HCl($v = 1$). Rather they were due to HCl in $v = 0$, $J = 0$ being ionized via a 2-photon resonance with $V^1\Sigma^+(v = 6)$, also reported by Rohlfing *et al.*[27] Comparing previous and current values of vibrational excitation probabilities (measured at similar incidence energies and temperatures) and the respective parameters derived from the fitting described in Section III (Eq. (5)), we found that the previous values are consistently lower than the current ones approximately by a factor of 50. This is also consistent with a comparison of the intensities of the transitions from $v = 0$ via the V and E states with the expected intensity of a thermal population in $v = 1$. Using this correction factor of 50, we include the previously reported vibrational excitation probabilities from Ref. 22 in the current analysis.

III. RESULTS AND ANALYSIS

Fig. 3 shows examples of REMPI spectra of scattered HCl($v = 0,1,2$) resulting from the inelastic channels: $v = 0 \rightarrow 1$ (columns 1 and 2) and $v = 1 \rightarrow 2$ (columns 3 and 4). Here, the incidence translational energy was $E_i = 0.64$ eV and T_S was 323, 593, and 953 K. All spectra have been corrected for detector gain and laser power. The strong increase in the REMPI signal from the respective upper vibrational state, $v = 1$ for $v = 0 \rightarrow 1$ and $v = 2$ for $v = 1 \rightarrow 2$, with increasing surface temperature is clearly observable. Additionally, it can be seen that the upper state signal with respect to the corresponding lower state signal is stronger for $v = 1 \rightarrow 2$. After correcting for small differences in scattering angular distributions, temporal dilution and state specific REMPI sensitivity, as described in detail in Ref. 28, we obtained the vibrational excitation probabilities from the ratio of REMPI signals for different HCl vibrational states. Since the incident beam largely consists of HCl in $v = 0$ (the $v = 1$ population is lower than our detection limit) and excitation probabilities for $v \geq 2$ are negligibly small, the HCl($v = 0 \rightarrow 1$) excitation probability can be approximated as

$$P_{0,1} = \frac{N_{0\rightarrow1}}{\sum_i N_{0\rightarrow i}} \approx \frac{N_{0\rightarrow1}}{N_{0\rightarrow0} + N_{0\rightarrow1}} \approx \frac{N_1}{N_0 + N_1}. \quad (3)$$

Here, N_i denotes the integrated REMPI signals (corrected for laser power, detector gain etc. as described in Ref. 28) that are proportional to the population of the corresponding vibrational state. For HCl($v = 1 \rightarrow 2$) excitation, we only consider the $v = 1$ population in the incident beam produced by laser excitation, and we ignore the (dominant) $v = 0$ population. HCl($v = 0 \rightarrow 1$) excitation could not be observed in the measurements of $P_{1,2}$ due to the low detector gain used for recording HCl($v = 1$) REMPI spectra, and thus did not influence our results. In addition, we only consider the $v = 1 \rightarrow 1,2$ channels, neglecting $v = 1 \rightarrow 0$ (which we cannot detect) and $v \geq 3$ (which is negligibly small),

$$P_{1,2} = \frac{N_{1\rightarrow2}}{\sum_i N_{1\rightarrow i}} \approx \frac{N_{1\rightarrow2}}{N_{1\rightarrow0} + N_{1\rightarrow1} + N_{1\rightarrow2}} \approx \frac{N_{1\rightarrow2}}{N_{1\rightarrow1} + N_{1\rightarrow2}} \approx \frac{N_2}{N_1 + N_2}. \quad (4)$$

One should note that we cannot measure the contribution of the $v = 1 \rightarrow 0$ channel due to the large HCl($v = 0$) background

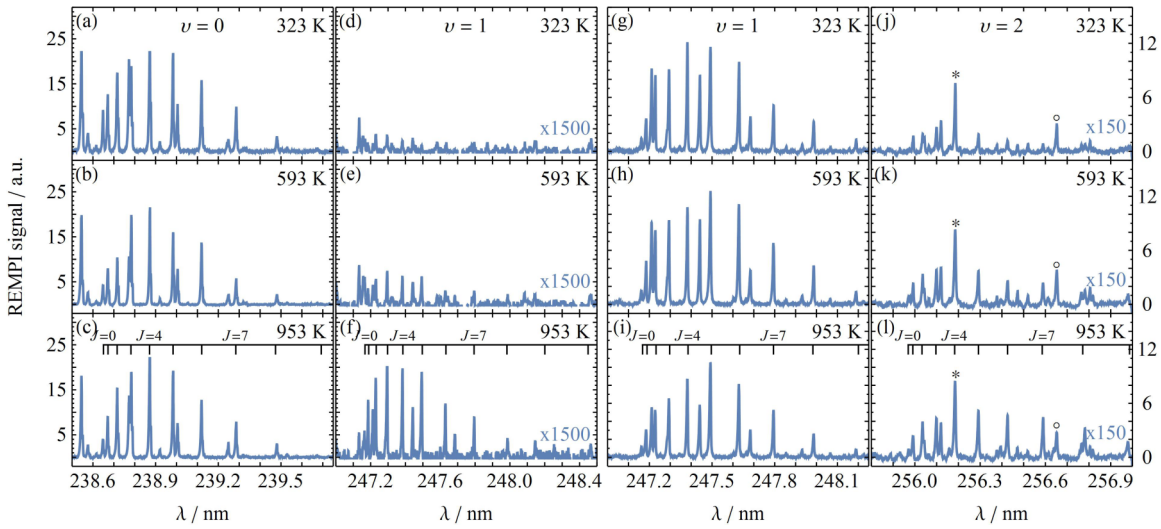

FIG. 3. HCl scattering channels $v = 0 \rightarrow 1$ (left two columns) and $v = 1 \rightarrow 2$ (right two columns). REMPI spectra of the scattered molecules in vibrational states $v = 0$ and 1 and $v = 1$ and 2, respectively, at a surface temperature of ((a), (d), (g), and (j)) 323 K, ((b), (e), (h), and (k)) 593 K and ((c), (f), (i), and (l)) 953 K with $E_i = 0.64$ eV. All spectra in one column were recorded under the same experimental conditions (except for T_S). While the change in the respective lower state intensities is almost negligible, the increase in the respective upper state intensity for higher surface temperatures is clearly seen. The spectra are corrected for laser power and detector gain. For the sake of visualization, the upper state spectra are multiplied by a factor of 1500 and 150, respectively. Additionally, two lines with temperature independent intensities not stemming from transitions of $v = 2$ via the $E^1\Sigma^+$ state are marked with an asterisk and a circle in the right-hand column. The former overlaps with the $J = 4$ line of $v = 2$.

produced by vibrationally elastic ($v = 0 \rightarrow 0$) scattering of the incident molecular beam. We justify this approximation as follows: Analysis of previously conducted measurements (unpublished results) showed that the relaxation probability for HCl($v = 2 \rightarrow 1$) at similar incidence energies is less than 0.3. As is shown below, vibrational excitation is strongly enhanced by incidence vibration. Assuming the same is true for vibrational inelasticity in general, we expect the probability for the HCl($v = 1 \rightarrow 0$) relaxation to be smaller than for HCl($v = 2 \rightarrow 1$). Even if relaxation probabilities were the same (i.e., 0.3 for both incidence vibrational states $v_i = 1$ and 2), our analysis would overestimate the vibrational excitation probabilities by approximately 30%.

The vibrational excitation probabilities derived in this manner are shown in Fig. 4. The results from the present work are shown as solid symbols. The open symbols are the results from Ref. 22, scaled with a constant factor of 50 to account for the incorrect calibration used previously (see Section II C). After scaling, old and new values are in reasonable agreement and can both be considered in further discussion. The excitation probabilities increase with surface temperature as well as with incidence translational energy. Moreover, the vibrational excitation probabilities for $v = 1 \rightarrow 2$ for the same incidence energy are generally about 20 times larger than for $v = 0 \rightarrow 1$.

The solid lines in Fig. 4 are the results of a simple fitting procedure that allows us to decompose the probabilities into two different contributions, which we now describe. Studies of vibrational excitation and its dependence on incidence translational energy and surface temperature show that two mechanisms of vibrational excitation are possible in the HCl/Au system:[22] electronically adiabatic (T-V) coupling and electronically nonadiabatic (EHP-V) coupling. For a system with both mechanisms active, the dependence on incidence translational energy and surface temperature can be described

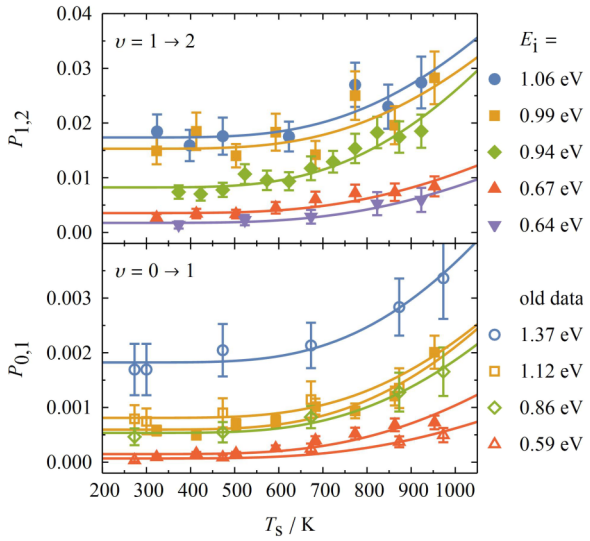

FIG. 4. Vibrational excitation probabilities for $v = 1 \rightarrow 2$ (upper panel) and $v = 0 \rightarrow 1$ (lower panel) as a function of surface temperature, for different incidence translational energies. Solid lines represent the fitted functions $P_{v,v'}$ (Eq. (7)). In the lower panel, the previously published data,[22] corrected as described in the text, are depicted with open symbols for comparison (see text for discussion).

by Eq. (5),

$$P_{v,v'}(E_i, T_S) = A^{ad.}_{v,v'}(E_i) + A^{nonad.}_{v,v'}(E_i) \exp\left(-\frac{E_{v,v'}}{k_B T_S}\right). \quad (5)$$

Here, k_B is the Boltzmann constant and $E_{v,v'}$ is the energy spacing between the vibrational states ($E_{1,2} = 0.342$ eV and $E_{0,1} = 0.358$ eV). The first fitting parameter, $A^{ad.}_{v,v'}(E_i)$, represents the T-V coupling which does not depend on surface temperature. The second term represents the EHP-V coupling, which depends on the thermal population of EHPs with enough energy to excite a vibrational transition —described by the exponential term. The intrinsic coupling strength between the EHPs of the metal and the molecular vibration, which in the high-temperature limit is equal to the nonadiabatic contribution to the vibrational excitation probability, is represented by the second fitting parameter, the translational incidence energy dependent pre-exponential factor $A^{nonad.}_{v,v'}(E_i)$.[32,33] By fitting the probabilities shown in Fig. 4, we can determine $A^{ad.}_{v,v'}(E_i)$ and $A^{nonad.}_{v,v'}(E_i)$ at a variety of incidence translational energies, decomposing the observed vibrational excitation probabilities into electronically adiabatic and nonadiabatic contributions. This approach has the advantage that the intrinsic coupling strength is independent of the surface temperature dependent population of hot electron-hole pairs that drives the nonadiabatic vibrational excitation.[32] This allows us to compare the adiabatic and nonadiabatic contributions on an even footing.

Fig. 5 shows the incidence translational energy dependence of the derived adiabatic and nonadiabatic parameters while Table II shows the corresponding numerical values. For the range of translational energies studied here, both $A^{ad.}_{v,v'}$ and $A^{nonad.}_{v,v'}$ increase linearly with E_i. To quantify this increase, the slopes $\partial A^{ad.}_{v,v'}/\partial E_i$ and $\partial A^{nonad.}_{v,v'}/\partial E_i$ of linear fits to the data (dashed lines in Fig. 5) are determined; see Table III.

We highlight three important observations arising from this analysis.

(1) The electronically nonadiabatic A-factor is larger than the adiabatic A-factor for all E_i used in this work. That is, the nonadiabatic interaction is stronger than the adiabatic interaction if one accounts for the population of hot EHPs needed for the nonadiabatic vibrational excitation, which is small under all conditions of this work, $\exp\left(-\frac{E_{v,v'}}{k_B T_S}\right) \ll 1$.

(2) At a constant incidence translational energy there is a strong enhancement of vibrational excitation in going from $v_i = 0$ to $v_i = 1$. Comparing the incidence energy independent derivatives in Table III, one finds that for $v_i = 1$ the adiabatic mechanism is enhanced by a factor of 24 when compared to $v_i = 0$. For the electronically nonadiabatic mechanism, the enhancement is by a factor of 9. That is, the increase in initial vibrational energy enhances the T-V energy transfer more than the EHP-V energy transfer.

(3) Following the two previous observations, an obvious next step was extending the comparison to higher initial vibrational states to examine a possible further increase in vibrational excitation probabilities. Thus, we excited incident HCl molecules into $v = 2$, $J = 1$ prior

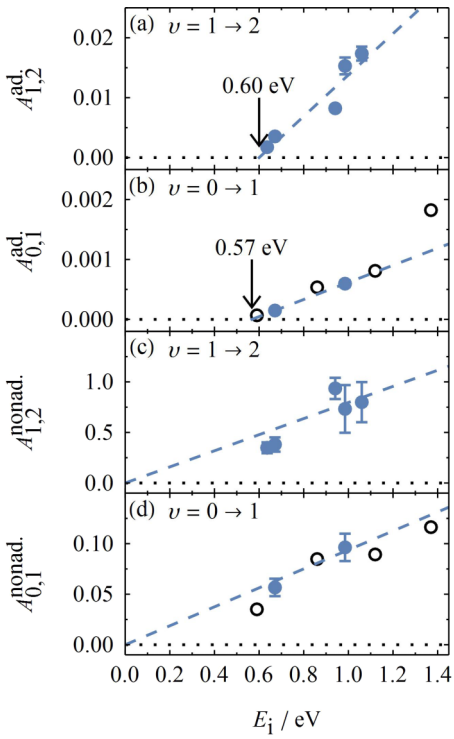

FIG. 5. E_i dependence of the electronically adiabatic and nonadiabatic pre-factors of the vibrational excitation for ((a) and (c)) $\upsilon = 1 \rightarrow 2$ and ((b) and (d)) $\upsilon = 0 \rightarrow 1$. Open circles are data from Ref. 22, corrected as described in the text. Note the order-of-magnitude difference between $\upsilon = 0 \rightarrow 1$ and $\upsilon = 1 \rightarrow 2$ excitation for both adiabatic and nonadiabatic pre-factors. The dashed lines denote linear fits to the new data of this study which allow derivatives with respect to incidence translational energy to be calculated. In (a) and (b), incidence translational energy thresholds for adiabatic excitation are indicated by arrows. In (c) and (d), the y-axis intercept was fixed at zero.

to collision. However, no signal from the vibrational excitation channel HCl($\upsilon = 2 \rightarrow 3$) could be observed.

Based on our detector gain range and a comparison to the observed excitation channels, we can give an estimate of the upper limit of HCl($\upsilon = 2 \rightarrow 3$) excitation probabilities. Assuming the same relative vibrational state detection sensitivities for $\upsilon = 2,3$ as for $\upsilon = 1,2$ and similar laser power

TABLE II. Overview of the adiabatic and nonadiabatic A-factors at different incidence translational energies.

E_i/eV($\upsilon \rightarrow \upsilon'$)	$A^{ad.}_{\upsilon,\upsilon'}$	$A^{nonad.}_{\upsilon,\upsilon'}$
$1.06(1 \rightarrow 2)$	1.7×10^{-2}	8.0×10^{-1}
$0.99(1 \rightarrow 2)$	1.5×10^{-2}	7.3×10^{-1}
$0.94(1 \rightarrow 2)$	8.2×10^{-3}	9.4×10^{-1}
$0.67(1 \rightarrow 2)$	3.5×10^{-3}	3.8×10^{-1}
$0.64(1 \rightarrow 2)$	1.7×10^{-3}	3.5×10^{-1}
$0.99(0 \rightarrow 1)$	6.0×10^{-4}	9.6×10^{-2}
$0.67(0 \rightarrow 1)$	1.5×10^{-4}	5.7×10^{-2}
$1.37(0 \rightarrow 1)$[a]	1.8×10^{-3}	1.2×10^{-1}
$1.12(0 \rightarrow 1)$[a]	8.1×10^{-4}	8.9×10^{-2}
$0.86(0 \rightarrow 1)$[a]	5.4×10^{-4}	8.5×10^{-2}
$0.59(0 \rightarrow 1)$[a]	6.8×10^{-5}	3.5×10^{-2}

[a]These are the previously published data from Ref. 22, now up-scaled by a factor of 50 as described above.

TABLE III. Dependence of adiabatic and nonadiabatic A-factors on incidence translational energy.

$\upsilon \rightarrow \upsilon'$	$\frac{\partial A^{ad.}_{\upsilon,\upsilon'}}{\partial E_i}$/eV^{-1}	$\frac{\partial A^{nonad.}_{\upsilon,\upsilon'}}{\partial E_i}$/eV^{-1}
$0 \rightarrow 1$	1.4×10^{-3}	9.4×10^{-2}
$1 \rightarrow 2$	3.4×10^{-2}	8.0×10^{-1}
$0 \rightarrow 1$ (NO)[a]	...	0.88
$2 \rightarrow 3$ (NO)[b]	...	1.6

[a]Calculated based on the values in Ref. 28.
[b]Calculated based on unpublished data for one incidence energy of 0.41 eV, see Sec. III of the supplementary material. This value was obtained from a linear fit through a single data point, with y-axis intercept fixed at zero, which is equivalent to $A^{nonad.}_{\upsilon,\upsilon'}/E_i$.

dependencies, we should have observed signal in $\upsilon = 3$ if the $\upsilon = 2 \rightarrow 3$ excitation probability was on the order of 0.05 or above ($E_i = 0.99$ eV, $T_S = 923$ K). That is, the increase in vibrational excitation probabilities going from $\upsilon = 1 \rightarrow 2$ to $\upsilon = 2 \rightarrow 3$ must at least be much less pronounced than going from $\upsilon = 0 \rightarrow 1$ to $\upsilon = 1 \rightarrow 2$. It seems likely that trajectories potentially leading to vibrational excitation as high as $\upsilon = 3$ lead to dissociation instead.

While further theoretical work is needed to more thoroughly understand this system, we hypothesize a qualitative explanation of the observed increase in vibrational excitation with increasing υ_i. The increased incidence vibrational energy allows scattering to occur via trajectories that sample geometries near a late transition state of HCl dissociation on Au(111) and when such trajectories fail to react, they result in enhanced vibrational excitation. Interestingly, recently reported time-dependent density functional theory based molecular dynamics simulations of a similar system, HCl scattering from Al(111), showed that the nonadiabatic effects are enhanced by vibrational excitation.[34] This increase was attributed to a large energy shift of the antibonding lowest unoccupied molecular orbital of HCl with increasing bond length, leading to a stronger interaction with the continuum of states of the metal. It could well be possible that the bond length increase in the vicinity of transition state configurations leads to an increase in the nonadiabatic interaction strength in this case, too.

This hypothesis is strengthened by comparing to another system, where vibrationally inelastic scattering has been intensively studied: NO scattering from Au(111), whose vibrational energy transfer is dominated by EHP-V coupling.[28] In previous studies of that system, incidence translational and vibrational energies comparable to those presented in this work were used. More precisely, the highest E_i and υ_i studied in measurements involving vibrational excitation were 1.05 eV and $\upsilon_i = 2$ (corresponding to a vibrational energy of 0.46 eV), respectively.[25,28] We note that the dissociation barrier of NO on Au(111) has been calculated by DFT methods to be higher than 3 eV.[24] Specifically, in Fig. 6 we compare the surface-temperature dependence of the NO($\upsilon = 0 \rightarrow 1$)[28,32] and NO($\upsilon = 2 \rightarrow 3$)[35] channels at $E_i = 0.41$ eV to the HCl($\upsilon = 0 \rightarrow 1$) and HCl($\upsilon = 1 \rightarrow 2$) at 0.67 eV.[36] One can immediately see that the incidence vibrational energy dependence is much stronger for HCl than for NO. For a quantitative comparison, the $\partial A^{nonad.}_{\upsilon,\upsilon'}/\partial E_i$ values for NO/Au(111) are also given in Table III. Here,

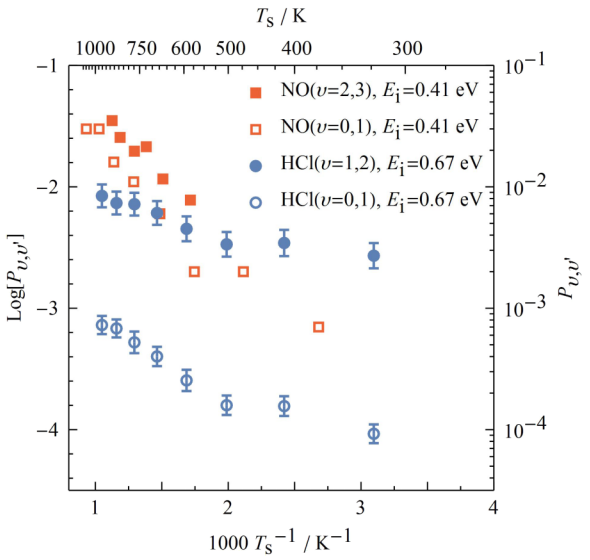

FIG. 6. Comparison of vibrational excitation probabilities for HCl/Au(111) for $v = 0 \rightarrow 1$ (blue open circles) and $v = 1 \rightarrow 2$ (blue filled circles) and NO/Au(111)[28,32] for $v = 0 \rightarrow 1$ (red open squares) and $v = 2 \rightarrow 3$ (red filled squares)—see Sec. III of the supplementary material. Increased incidence vibrational energy shows a much larger effect on the vibrational inelasticity in the case of HCl, where a transition state for dissociation is presumably accessible under the studied conditions (E_i, v_i). Note that the factor between NO($v = 2 \rightarrow 3$) and NO($v = 0 \rightarrow 1$) is ~2 while the factor between HCl($v = 1 \rightarrow 2$) and HCl($v = 0 \rightarrow 1$) is ~10-30 depending on the surface temperature.

one can see that for NO the enhancement for $v_i = 2$ in comparison with $v_i = 0$ ($E_{0,2} = 0.46$ eV) is only by a factor of less than 2, whereas it is a factor of 9 for $v_i = 1$ versus $v_i = 0$ ($E_{0,1} = 0.36$ eV) in the case of HCl. Thus it appears likely that for NO/Au(111) the barrier to dissociation is too high to play a role in the vibrational excitation. For HCl/Au(111), where the barrier is lower, vibrational excitation is considerably enhanced by the incidence vibrational state, suggesting that the transition state to dissociation might well influence vibrationally inelastic scattering events.

IV. CONCLUSIONS AND SUMMARY

In summary, our results suggest that vibrational excitation of HCl on Au(111) is a sensitive probe of the reactive transition state for dissociation on the surface. We find concurrent adiabatic (T-V) and nonadiabatic (EHP-V) mechanisms of excitation to occur for the $v = 1 \rightarrow 2$ channel. Additionally, based on new measurements of the $v = 0 \rightarrow 1$ excitation probabilities with improved calibration for the detection sensitivities, we were able to correct previously reported erroneous values and include them for comparison. Our results show that initial vibrational energy increases the probability for further vibrational excitation. In comparison to $v = 0 \rightarrow 1$, the probability for $v = 1 \rightarrow 2$ vibrational excitation probability is 20 times higher. The $v = 2 \rightarrow 3$ vibrational excitation channel could not be observed—presumably because the majority of these trajectories lead to dissociation instead of further vibrational excitation. This is in line with our recent findings on the dissociation of HCl on Au(111) which suggest that molecules in $v = 1$ are more reactive than those in $v = 0$.[17] We believe that these results present valuable benchmark data for testing future theoretical approaches to this system, particularly with regard to modelling the dissociative transition state.

SUPPLEMENTARY MATERIAL

See supplementary material for further details regarding the relative sensitivity factors, time-of-flight data and analysis, determination of NO/Au(111) vibrational excitation probabilities, and angular distributions.

ACKNOWLEDGMENTS

We acknowledge support from the Deutsche Forschungsgemeinschaft CRC1073 under Project No. A04 and from the Ministerium für Wissenschaft und Kultur Niedersachsen and the Volkswagenstiftung under Grant No. INST 186/901-1. A.M.W. and P.R.S. acknowledge support from the Alexander von Humboldt Foundation. J.G. acknowledges support from the Max-Planck—EPFL Center for Molecular Nanoscience and Technology. I.R. and A.M.W. acknowledge support from the Niedersächsisch-Israelische Gemeinschaftsvorhaben under Project No. 574 7 022.

The authors would also like to thank Dr. Daniel J. Auerbach for his helpful suggestions throughout the course of the work and Professor Dirk Schwarzer for providing the nozzle.

[1]M. Born and R. Oppenheimer, Ann. Phys. **20**, 457 (1927).
[2]H. Eyring and M. Polanyi, Z. Phys. Chem. **227**, 1221 (2013).
[3]S. C. Althorpe and D. C. Clary, Annu. Rev. Phys. Chem. **54**, 493 (2003).
[4]J. M. Bowman and G. C. Schatz, Annu. Rev. Phys. Chem. **46**, 169 (1995).
[5]W. Hu and G. C. Schatz, J. Chem. Phys. **125**, 132301 (2006).
[6]S. Nave and B. Jackson, Phys. Rev. Lett. **98**, 173003 (2007).
[7]L. B. F. Juurlink, D. R. Killelea, and A. L. Utz, Prog. Surf. Sci. **84**, 69 (2009).
[8]K. Golibrzuch, N. Bartels, D. J. Auerbach, and A. M. Wodtke, Annu. Rev. Phys. Chem. **66**, 399 (2015).
[9]J. Behler, Phys. Chem. Chem. Phys. **13**, 17930 (2011).
[10]J. Behler, J. Phys.: Condens. Matter **26**, 183001 (2014).
[11]J. Behler, Int. J. Quantum Chem. **115**, 1032 (2015).
[12]S. M. Janke, D. J. Auerbach, A. M. Wodtke, and A. Kandratsenka, J. Chem. Phys. **143**, 124708 (2015).
[13]A. M. Wodtke, Chem. Soc. Rev. **45**, 3641 (2016).
[14]C. T. Rettner, D. J. Auerbach, and H. A. Michelsen, Phys. Rev. Lett. **68**, 2547 (1992).
[15]C. Díaz, R. A. Olsen, D. J. Auerbach, and G. J. Kroes, Phys. Chem. Chem. Phys. **12**, 6499 (2010).
[16]J. C. Polanyi, Acc. Chem. Res. **5**, 161 (1972).
[17]P. R. Shirhatti, J. Geweke, C. Steinsiek, C. Bartels, I. Rahinov, D. J. Auerbach, and A. M. Wodtke, J. Phys. Chem. Lett. **7**, 1346 (2016).
[18]T. Liu, B. Fu, and D. H. Zhang, Sci. China: Chem. **57**, 147 (2013).
[19]In Ref. 17 we have shown that the calculated barrier height might be too low. In any case, the time-of-flight data presented in the supplementary material show that approximately half the translational energy is lost to surface phonon excitation during the scattering process. Thus, the mean incident translational energies used in this study alone are not high enough to overcome the barrier.
[20]T. Liu, B. Fu, and D. H. Zhang, J. Chem. Phys. **139**, 184705 (2013).
[21]T. Liu, B. Fu, and D. H. Zhang, J. Chem. Phys. **140**, 144701 (2014).
[22]Q. Ran, D. Matsiev, D. J. Auerbach, and A. M. Wodtke, Phys. Rev. Lett. **98**, 237601 (2007).
[23]Q. Ran, D. Matsiev, A. M. Wodtke, and D. J. Auerbach, Rev. Sci. Instrum. **78**, 104104 (2007).
[24]H. Falsig, J. Shen, T. Khan, W. Guo, G. Jones, S. Dahl, and T. Bligaard, Top. Catal. **57**, 80 (2014).
[25]K. Golibrzuch, P. R. Shirhatti, J. Altschaffel, I. Rahinov, D. J. Auerbach, A. M. Wodtke, and C. Bartels, J. Phys. Chem. A **117**, 8750 (2013).

[26]W. R. Simpson, T. P. Rakitzis, S. A. Kandel, A. J. Orr-Ewing, and R. N. Zare, J. Chem. Phys. **103**, 7313 (1995).
[27]E. A. Rohlfing, D. W. Chandler, and D. H. Parker, J. Chem. Phys. **87**, 5229 (1987).
[28]R. Cooper, Z. Li, K. Golibrzuch, C. Bartels, I. Rahinov, D. J. Auerbach, and A. M. Wodtke, J. Chem. Phys. **137**, 064705 (2012).
[29]K. Golibrzuch, P. R. Shirhatti, I. Rahinov, D. J. Auerbach, A. M. Wodtke, and C. Bartels, Phys. Chem. Chem. Phys. **16**, 7602 (2014).
[30]I. Rahinov, R. Cooper, C. Yuan, X. Yang, D. J. Auerbach, and A. M. Wodtke, J. Chem. Phys. **129**, 214708 (2008).
[31]C. T. Rettner, J. Chem. Phys. **101**, 1529 (1994).
[32]D. Matsiev, Z. Li, R. Cooper, I. Rahinov, C. Bartels, D. J. Auerbach, and A. M. Wodtke, Phys. Chem. Chem. Phys. **13**, 8153 (2011).
[33]D. M. Newns, Surf. Sci. **171**, 600 (1986).
[34]M. Grotemeyer and E. Pehlke, Phys. Rev. Lett. **112**, 043201 (2014).
[35]Based on previously unpublished data for NO/Au(111) $v = 2 \rightarrow 3$ excitation. Data, analysis, and further comparison are given in Section III of the supplementary material.
[36]Unfortunately we do not have data for exactly the same incidence translational energy. Since we approximatively determine the derivative of the nonadiabatic A-factor with respect to the incidence translational energy in Table III, this comparison should still be valid.